Original Article

Nano-Zinc Oxide Induced Pancreatic Toxicity and the Ameliorating Role of Naringenin: Histological and Immunohistochemical Study

Amal S. Sewelam and Mohammed Ahmed Shehata Amin

Department of Human Anatomy and Embryology, Faculty of Medicine, Zagazig University, Egypt

ABSTRACT

Background: Though Nano-zinc oxide particles (ZnO NPs) are widely applied in biomedicine, bioengineering and cosmetology, a controversy developed between ZnO NPs benefits versus toxicity on biological systems. Naringenin is a natural antioxidant flavonoid.

Objective: To explore the histological and immunohistochemical alterations in the rat pancreas following intraperitoneal exposure to two different doses of 35 nm ZnO NPs and to assess the ameliorating role of Naringenin.

Materials and Methods: Forty-five adult male rats were split randomly into five groups. Group1 served as control. Groups2 and 4 received a single intraperitoneal injection of 250 and 700 mg/kgbw ZnO NPs. Groups3 and 5 administered ZnO NPs as previously described followed by Naringenin gavaged at a dose of 20mg/kgbw/day once daily for 14 consecutive days. Histological, immunohistochemistry, biochemistry, and morphometry studies were accessed in the pancreatic tissue gained from all animals under the study.

Results: Contrasted to the group of control, ZnO NPs exhibited a dose dependent pancreatic tissue and cellular damage manifested as vascular congestion, duct dilatation, fibrosis, and inflammatory cell infiltration. Also, both acinar and B-cells showed degenerating changes varied from just cytoplasmic vacuolization in the ZnO NPs(250mg)-treated rats to severe cell shrinking, pyknosis, cytoplasmic and nuclear fragmentation in the ZnO NPs(700mg)-treated rats. Moreover, ZnO NPs provoked significantly increased mean area percentage of collagen fiber deposition and caspase immunoexpressing, significantly raised fasting blood glucose, serum amylase, lipase and MDA levels besides significant decline regarding insulin immunoexpressing. Naringenin administration induced a great recovery concerning the ZnO NPs (250mg)-treated rats but partial recovery regarding the ZnO NPs (700mg)-treated rats.

Conclusion: ZnO NPs potentially persuaded an oxidating stress manifest as structural and functional toxicity in the rat pancreas with great reversibility by Naringenin coadministration. A future work concerning ZnO NPs toxicity on vital organs and Naringenin role in opposing this impact is recommended.

Received: 27 December 2020, **Accepted:** 25 January 2021

Key Words: Naringenin; pancreas; zinc oxide nanoparticles.

Corresponding Author: Amal S. Sewelam, Department of Human Anatomy & Embryology, Faculty of Medicine, Zagazig University, Egypt, **Tel.**: +201 155789552, **E-mail:** amalsolimansewelam@gmail.com, ASSoeilam@medicine.zu.edu.eg

ISSN: 1110-0559, Vol. 44, No.4

INTRODUCTION

Zinc oxide nanoparticles (ZnO NPs) are considered the greatest properly utilized metal NPs in industry, cosmetology, diagnostics, medicine, chemistry and in microelectronics. They are of an increasing need in biomedicine and bioengineering due to their high stability, low cost, intrinsic photoluminescence characteristics and semiconductor properties[1].

Due to efficient UV absorptive properties, ZnO NPs are increasingly applied in personal care products like make-ups and sunscreen lotions. Also, they have many industrial applications such as dyes, paints, pigments and electronics[2-4]. Besides, ZnO NPs are used as food additives and in food packaging due to their antimicrobial performance[5] and have a good photocatalytic activity for organic pollutants in water[6]. More attention has been paid to ZnO NPs due to considered anticancer properties[7,8]. Human exposure to ZnO NPs can occur via oral ingestion, dermal penetration, intravenous injection, and inhalation[9-11].

In the last few years, ZnO NPs use became questionable. Though simply passing through cell membrane, interacting with cell macromolecules, and producing therapeutic effects on some organs, they were found to cause oxidative stress and cytotoxic influence in other organs[12].

Experimental animal studies revealed that, in rats, the spleen, liver, pancreas, heart, and bone were target organs for 20-nm ZnO NPs toxicity upon oral exposure[13]. Also, 35-nm ZnO NPs intraperitoneal exposure led to structural and functional hepatotoxicity owing to their potential oxidating stress[14]. Moreover, orally taken 15-nm ZnO NPs could result in increased blood glucose level, severe anemia and marked histopathological changes in the hepatic and cardiac tissues[15]. In the same context, oral intake of a high dose of ZnO NPs resulted in pancreatitis and anemia[16] and caused squamous and glandular cell hyperplasia in

 DOI: 10.21608/ejh.2021.55443.1405

the stomach and acinar cell apoptosis in the pancreas[17]. Similarly, ZnO NPs gavaged to rats, adversely altered the hematological indices and led to histopathological changes in the spleen, stomach, and pancreas[18] and resulted in oxidative stress, genotoxicity, inflammatory response, and apoptosis in rat's brain[19]. Moreover, ZnO NPs inhalation exerted tracheobronchial and alveolar inflammation[20]. Oral and intraperitoneal (IP) administration of 100 nm ZnO NPs resulted in liver, spleen, kidney, and lung toxicity[21] and histopathological changes in the rat brain and spinal cord[22].

The potential Zinc oxide NPs injurious impact was primarily concerned with their high solubility and oxidating stress inducing ability. In addition, whole NPs sizes can induce free radicals generation with a harmful influence at the tissue, cellular and macromolecular level since smaller NPs sizes are more hazardous than the larger ones[23,24]. Furthermore, 50–70 nm ZnO NPs exposure can persuade forcible but reversible inflammatory reaction meanwhile NPs of 10 nm size resulted in granulomatous inflammation[9].

Naringenin (NRG) is a natural flavonoid widely distributed in citrus fruits, tomatoes, cherries, grapefruit, and cocoa[25]. Several studies have proved that, NRG has so many protective effects and it can be applied as anticarcinogenic[26] anti-inflammatory[27] antioxidant[28], anti-diabetic[29], and hepatoprotective[30].

It is predictable that the ZnO NPs venture will be increased and human body will be more liable to NPs exposure via numerous varying routes such as ingestion, inhalation and skin contact. In accord with the fast progressive usage and marketing of ZnO NPs, an alarm has been growing concerning their toxicity. The data regarding ZnO NPs potential hazards about human well-being is restricted with a prerequisite to be well investigated with special consideration regarding different human tissues, cells, and macromolecules.

Up to our knowledge, inadequate information is obtainable on the histological and immunohistochemical changes induced by ZnO NPs on the vital organs. Therefore, the present study was assumed to clarify the alterations that might be persuaded by two different doses of these particles in the pancreatic tissues and to explore the possible preventive role of NRG. Consequently, ZnO NPs exposure could be controlled by daily consuming foods containing flavonoids.

MATERIALS AND METHODS

Chemicals

The chemicals used in this study were manufactured by Sigma-Aldrich, a chemical company, USA, and purchased from Sigma-Egypt.

1- Zinc oxide nanoparticles

white odorless fine powder obtained in glass bottles, each contained 5 gm and have the following characterizations (in accord with the manufacturer's specification); CAS Registry Number (CASRN), 677450; Average Particle Size (APS), 35 nm; approximately spherical in shape; purity >97%; surface area >10.8 m^2/g.

For dosage preparation, the powdered ZnO NPs were well dispersed in sterile acidic distilled water with a pH 5.5 because ZnO NPs are rapidly dissolved in acidic condition. The solution was homogenized by sonication using Misonix Sonicator, 55 W. Sonication occurred 10 times, each for 30 seconds with 2 minutes interval to make a stock solution with a concentration of 500mg ZnO NPs/ mL distilled water. From this suspension, the two required doses; 250 mg/kgbw and 700mg/kgbw of ZnO NPs were obtained for (IP) injection. Immediately before use, the NPs were vortexed 5 times for 10 seconds at 37◦ C to confirm a uniform suspension[14,31,32].

2-Naringenin (NRG)

White odorless fine powder obtained in glass bottles each contained 1 gm with CASRN 5893. After dissolving in distilled water, it was gavaged in a dose of 20mg/kgbw once daily for 14 successive days according to[25]. These procedures were performed in ZSMRC (scientific medical research center) at the Faculty of Medicine, Zagazig University (ZU).

A*nimals and Experimental Design*

The present study was conducted on apparently healthy adult male albino rats (n=45, 8-week-old, 190–220gmbw) brought from ZSMRC. This study was carried out in accord with the ethics committee of ZU. All procedures involving the rats used were reviewed and approved by the Institutional Animal Care and Use Committee, ZU (ZU-IACUC) with an approval number (ZU-IACUC/3/F/39/2020).

The animals were kept in a clean place, housed in stainless-steel cages under environmentally standard laboratory conditions (25-27 °C,12 h-dark / light period, and relative humidity of 50 ± 5%) until the experiment end. The animals were permitted to access freely commercial food (standard rodent food pellet, tap water ad libitum). One week of acclimation to the climate conditions was allowed for rats prior to the beginning of the study procedures.

The rats were allocated randomly into five main experimental groups, (n=9/group).

Group1: served as control group, were allowed to feed and drink normally with no addition to any material or drug in their diet. The rats were equally subdivided into 3 subgroups, (n=3/subgroup). Subgroup 1a (negative control): rats were kept with no treatment but received a balanced diet. Subgroup 1b (positive control): were gavaged NRG at a dose of 20mg/kgbw once daily for 2 successive weeks. Subgroup 1c (vehicle subgroup): were injected 1ml of sterile acidic distilled water (PH=5.5) at 37◦ C IP once only for equivalency of shock resulting from the (IP) injection.

Group2: ZnO NPs (250mg-treated rats) received a single (IP) injection of a low toxic dose of ZnO NPs (250 mg/kgbw) then left without medication for succeeding 2weeks.

Group3: ZnO NPs (250mg-treated rats) +NRG administered a single (IP) injection of a low toxic dose of ZnO NPs (250 mg/kgbw) followed by a daily oral dose of NRG (20mg/kgbw) for 14 consecutive days.

Group4: ZnO NPs (700mg)-treated rats received a single (IP) injection of a high toxic dose of ZnO NPs (700 mg/kgbw) then received no medication for following 2 weeks.

Group5: ZnO NPs (700mg) + NRG treated rats administered a single (IP) injection of a high toxic dose of (ZnO NPs (700 mg/kgbw) followed by a daily oral dose of NRG (20mg/kgbw) for 14 consecutive days.

All animals were kept under observation through the experiment for any mortality. During the last day of the experiment, animals were deprived of food overnight and then anesthetized by an (IP) injection of thiopental (50 mg/kgbw)[33].

After anesthesia, blood samples from the retro-orbital plexus, 3ml from each rat, using capillary glass tubes[34] were taken just before termination for biochemical valuation. Then, a midline laparotomy was done, the pancreas was dissected out, excised immediately, subdivided into two portions. One slice was fixed in 10% neutral buffered formalin overnight then handled to obtain paraffin blocks. The other part of the pancreas was prepared to get tissue homogenate for estimation of Malondialdehyde (MDA) level.

A-Biochemical assessment

1-Measurement of fasting blood glucose (FBG), serum amylase and lipase levels.

Before rat termination, 8 hours after food deprivation, tail vein blood samples were obtained and FBG was estimated using a blood glucometer (single touch pulse, Accu-Check Performa, German Roche Diagnostics). The obtained blood samples from the retro-orbital plexus were incubated at 25°C, left undisturbed for 30 minutes till clotting before centrifuging at 3000 rpm for 15 minutes to separate the serum. The collected serum was kept until the time of assay for the estimation of serum amylase and lipase levels using appropriative diagnostic kits consistent with the manufacturer's directions (Diagnostic Systems, Germany)[35].

2-Preparation of tissue homogenate and MDA estimation.

Pancreatic tissue was prepared for MDA valuation, a lipid per oxidating parameter, by bathing with isotonic saline, crushing, homogenizing in 10% PBS (phosphate-buffered saline) then, sonicating (4 times for 30 sec., 20 sec., interval). The homogenate was subjected to centrifugation for 5 minutes at 10,000 rpm (-4˚C) to get rid of nuclei and debris. The supernatant was directly used to estimate MDA level spectrophotometrically in consistency with the methods of[36]. The mean values of serum amylase, lipase, and MDA levels were recorded.

B-Histological examination

The gained pancreatic tissue from all rats of both control and treated groups was fixed in 10% neutral buffered formalin overnight, then handled to obtain paraffin blocks by direct dehydration in a graded succession of ethanol then blocked-in paraffin wax.

Serial paraffin sections, 5 μm thickness, were prepared to be stained with hematoxylin and eosin (H&E) to check histological details and also with Masson Trichrome (MT) stain to verify the collagen fibers as stated by[37,38] respectively. Stained slides were inspected and photo'd in the unit of image analysis in the anatomy department, faculty of medicine, ZU via an ocular microscope (Lecia, ICC500 W", with a Leica digital camera).

C-Immunohistochemistry valuation

Immunohistochemistry was achieved to investigate Caspase-3 (apoptosis marker) and anti-insulin antibody immunoexpressing. The peroxidase-labeled Streptavidin Biotin Technique was used to accomplish immunohistochemical studies as stated by[39]. The Paraffin sections were subjected to the following subsequent steps; deparaffinization, rehydration down to distilled water, treatment with 3% dihydrogen dioxide (H_2O_2) for 5 minutes, rinsing with phosphate buffer solution (PBS) for 15 minutes, blocking with 1.5% normal goat serum in PBS and incubation with the primary antibody for 45 minutes at room temperature. For finding apoptosis, an anti-caspase-3 mouse monoclonal antibody (Dako Company, Cairo, Egypt, Catalog No. IMG-144A at a dilution 1/200) was used. To identify B-cells in Langerhans islets, the anti-insulin monoclonal mouse primary antibody (DAKO LSAB 2 Kit; Dako, Denmark) at a dilution of 1:100 was used. After that, the sections were incubated with a biotinylated antibody (biotin-conjugated goat anti-rabbit IgG, at a dilution of 1:200) for 1 hour, at room temperature. Then, rinsed in PBS, immersed into the chromogen diaminobenzidine for the reaction products visualization, and finally, counterstained with hematoxylin (H), dehydrated and covered. Slides stained with IgG (2ry antibody) were only utilized as negative controls.

D-Image analysis and morphometric study

The pancreatic sections stained by MT, sections marked by an anti-Caspase3 antibody as well as sections treated with anti-insulin antibody were subjected to morphometrical analysis using the image analyzer computer system (software Leica Quin 500) at the Oral Pathology Department, Dental Medicine College, Cairo University. It measures the area% of collagen fiber deposition and of caspase-3 protein immune expressing in pancreas tissue of

rats / unit area (Unit area means microscopic field) using a standardized measurement frame at a magnification x100 by light microscope transported to the screen of monitor. Also, it measures insulin immune expressing area % in the cytoplasm of B-cells of Langerhans islets. Area % values from pancreatic sections of rats in each experimental group were obtained. Five non-overlapping pancreatic sections from each rat in each studied group were examined at a magnification x100 and 10 readings were calculated[40]. At the same magnification, for each rat/group, the area % values of insulin immunoexpressing of at least 20 Langerhans islets were measured[41]. Values were presented as (mean ± SD) and were processed for statistical analysis.

E-Statistical analysis

The recorded mean values of serum amylase, lipase, and MDA levels and the collected morphometric data were computerized and statistically analyzed using Graph Pad Prism 5.01. Quantitative data were expressed as mean ± SD (Standard deviation). Differences between mean values of experimental groups were tested with analysis of variance (ANOVA). Tukey's multiple comparison test was carried out the post hoc test of ANOVA. Both ZnO NPs (250mg)-treated and ZnO NPs (700mg)-treated groups were compared to the control group. However, ZnO NPs (250mg)-treated +NRG group was compared to ZnO NPs (250mg)-treated group and ZnO NPs (700mg)-treated +NRG was compared to ZnO NPs (700mg)-treated group. The results were considered statistically significant when the *P value* <0.05. Different stages of significance were put into consideration. High significance (***) when *P value* < 0.001, Moderate significant (**) at 0.01 >*P value* >0.001 and low significance (*) when 0.01 > *P value* >0. 05.

RESULTS

There was no mortality in rats among ZnO NPs treated groups.

A- Histological alterations

Histological examination of all sections from rats of subgroups 1a, 1b, and 1c of the control group revealed no documented histological differences among the three subgroups. Thus, the results of subgroup 1a were selected to describe the control group.

Sections of the control rat pancreas stained with Hematoxylin and eosin displayed normal histological construction; formed of multiple varying sized and shaped lobules bound together by delicate interlobular connective tissue (CT) septae contained interlobular blood vessels and ducts. Each lobule appeared composed of the pancreatic acini; the exocrine part, and the Langerhans islets; the endocrine part, distributed among the acini. The Langerhans islets consisted of endocrine cell clusters with blood capillaries in-between (Figures 1a,b). The acinar cells appeared single-layered pyramidal cells having basal rounded vesicular nuclei. Their cytoplasm stained acidophilic near the acinar lumen but basophilic away from the lumen (Figure 1c).

However, concerning Group2, contrasting to the group of control, ZnO NPs administration in a low dose (250mg/kgbw) resulted in mild degenerative alterations mainly affecting the whole pancreatic lobules. They were manifested as thickened interlobular CT septae, mild vascular congestion with mild perivascular inflammatory cell infiltrate (Figure 2a). Also, the interlobular ducts were somewhat distended with mild periductal inflammatory cell infiltrate (Figure 2b). Most Langerhans Islets were apparently normal. However, mildly congested blood capillaries and few vacuolated islet cells were distinguished (Figure 2c). Some acini appeared merged, and the acinar cells exhibited cytoplasmic vacuolation and darkly stained nuclei (Figure 2d).

Fortunately, following NRG administration, pancreas sections from group3 revealed a great recovery when comparing with group2 with restoration of the pancreatic construction to become more or less similar to the group of control. The pancreatic lobules, the interlobular septae, blood vessels, and ducts, the acini, and the Langerhans islets revealed a great resemblance to the control group (Figures 3a-c).

Nevertheless, regarding Group4, ZnO NPs administered in a high dose(700mg/kgbw) resulted in massive destructive changes approximately disturbing the whole pancreatic lobules indicating severe toxicity when comparing with the other groups. The blood vessels were severely dilated and congested, and surrounded by thick CT. The pancreatic acini were apparently reduced in number (Figure 4a). The interlobular ducts were greatly distended, irregular, thin-walled and occasionally ruptured (Figure 4b). In certain areas of the pancreas, necrotic fat cell aggregates were visible (Figure 4c). Most cells of Langerhans islets exhibited vacuolated cytoplasm and small darkly stained nuclei. Other cells showed complete cytoplasmic lysis leaving empty spaces (Figure 4d).

The acini seemed severely degenerated, necrotic with disturbed cytoarchitecture. Diffuse interstitial inflammatory cell infiltration was well demonstrated (Figure 4e). Some acinar cells displayed cytoplasmic vacuolation and pyknotic nuclei. Other cells showed cytoplasmic lysis, nuclear flattening leaving wide acinar lumen containing necrotic exfoliate (Figure 4f). Other acinar cells presented cytoplasmic and nuclear fragmentation meanwhile other acini were severely shrunken (Figure 4g).

On the contrary, concerning Group5, NRG administration led to a partial recovery in the histological alterations of the pancreas, when contrasted to group 4. The blood vessels were less congested, and the ducts were less dilated. The interstitial inflammatory cell infiltrate was diminished and the acini were apparently increased in number. However, some acini were still demonstrating wide acinar lumina (Figure 5a). The Langerhans islets exhibited a great improvement. However, some islet cells were still showing cytoplasmic vacuolation. Some pancreatic acini restored normal acinar cytoarchitecture but the acinar cells

were still exhibiting cytoplasmic vacuolations and darkly stained nuclei. In the meantime, other acini demonstrated marked degenerative changes and appeared shrunken (Figures 5b,c).

On the other hand, MT staining sections of group1 revealed a small collagen fibers amount distributed around the interlobular ducts and blood vessels (Figure 6a). In rats of group2, contrasted to group1, the amount of collagen was mildly increased (Figure 6b). In group3, NRG administration led to a marked improvement comparable to group 2 and a small collagen fibers amount was distinguished with a distribution more or less similar to the group of control (Figure 6c). In group4, relative to other groups, extensively dense collagen was deposited around the interlobular ducts, and the blood vessels (Figure 6d). By NRG administration in group5, an improvement was observed and the collagen fiber deposition was markedly decreased comparable with group4 but still greater than that found in the control group (Figure 6e).

In addition, anti-insulin immunohistochemical staining sections of rat pancreas in group1 revealed a strong immunoreactivity (represented by deep brown coloration) of insulin in the cytoplasm of β-cells which occupied most of the Langerhans islets as presented in (Figure 7a) meanwhile mild decline in immunohistochemical expression was noticed in group 2 relative to group1 (Figure 7b). In group3, contrasted to group 2, the pancreatic β-cells showed strongly positive anti-insulin antibody staining with a deep brown color nearly like the group of control (Figure 7c). In group4, compared to other groups, immunohistochemical staining presented an evident decrease in insulin immune expressing in β-cells which stained light brownish coloration (Figure 7d), and in group 5, an apparent increase in insulin immunoexpressing in β-cells was observed when compared with group4 (Figure 7e). In all groups, non-B-cells showed no reaction.

Furthermore, anti-Caspase3 immunohistochemical stained pancreatic sections of rats in both groups1&3 revealed minimal immunoreactivity (represented by light brown coloration) in the cell cytoplasm of both islet and acinar cells as presented in (Figures 8a,c). Also, moderate immunoreactivity was noticed in both groups 2,5 (Figures 8b,e). In group4, contrasted to group1, a strongly positive reaction represented by deep brown color was observed (Figure 8d).

B-Statistical results

The mean area (%) of collagen fiber content and caspase immunoexpressing in group2 displayed a highly significant rise contrasted to group1.Then, showed a highly significant decline in the group3 compared to group2. Also, it was highly significantly raised in the group4 when comparing with group1 and became low significantly declined in group5 relative to group4. On the controversy, the mean area (%) of insulin immunoexpressing showed a highly significant decline in group2 when comparing with group1 then showed a low significant elevation in group3 relative to group2. Also, it presented a highly significant decline in group4 contrasted to group1and was low significantly raised in group5 relative to group4.

In conclusion, a high significant rise in the mean area (%) of collagen fibers and caspase immunoexpressing but a highly significant decline regarding insulin immunoexpressing in both groups2,4 comparing with group1 were recorded denoting ZnO NPs dose dependent toxicity.

However, after NRG administration, the mean collagen and caspase area (%) showed a high significant, low significant decrease in groups3&5 correspondingly but a low significant rise in both groups3&5 concerning insulin when contrasted to both groups2&4 respectively. This indicates great improvement with NRG in ZnO NPs (250mg-treated rats) but partial in ZnO NPs (700mg-treated rats) as shown in (Table 1, Histogram 1).

C-Biochemical results

Regarding FBG, serum amylase and lipase levels, and pancreatic MDA level, no significant variations between the rats of the subgroups 1a,1b, and 1c were recorded. Concerning FBG level, there was no significant variation between the control, ZnO NPs (250mg-treated rats) and ZnO NPs (250mg-treated rats)+NRG groups suggesting that the endocrine part of the pancreas was not predisposed by low ZnO NPs dose. However, in group4, administration of ZnO NPs in a high dose induced a high significant rise in FBG level contrasted to group1 but a low significant decline in group5 compared with group4.

Also, ZnO NPs administration resulted in a highly significantly elevated serum amylase and lipase levels, and pancreatic MDA level in both groups2&4 comparing with group1. NRG administration led to a high significant reduction in the group2 and a moderate significant decline in group4 as shown in (Table 2).

These results confirm ZnO NPs toxicity with a great recovery in ZnO NPs (250mg-treated rats) +NRG group but partial recovery concerning ZnO NPs (700mg-treated rats)+ NRG group.

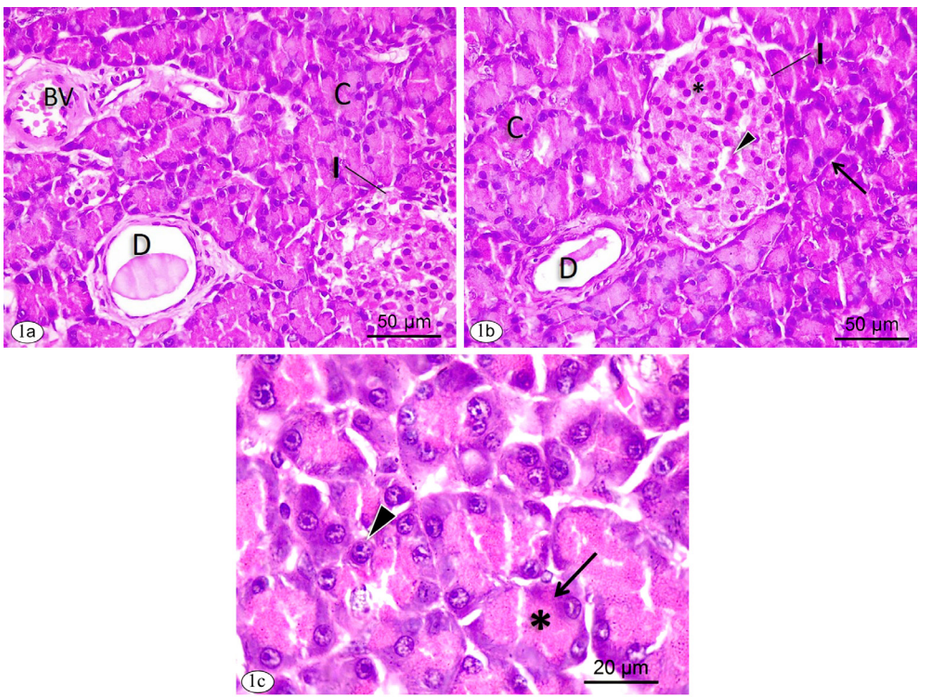

Fig. 1(a-c): Photomicrographs of a section of rat's pancreas of the control group (subgroup1a, negative control) demonstrating (a, b): the exocrine acini (C), the Langerhans islets(I) and the interlobular blood vessels (BV), duct (D) and CT septum (arrow). The Langerhans islets(I) appear composed of clusters of endocrine cells (*) with blood capillaries (arrowhead) in-between. (c): the pancreatic acini appear lined with pyramidal cells having basal rounded vesicular nuclei (arrowhead). Their cytoplasm stained basophilic away from the acinar lumen (arrow) and acidophilic near the lumen (*) (H&E. a & b x400, c=x1000).

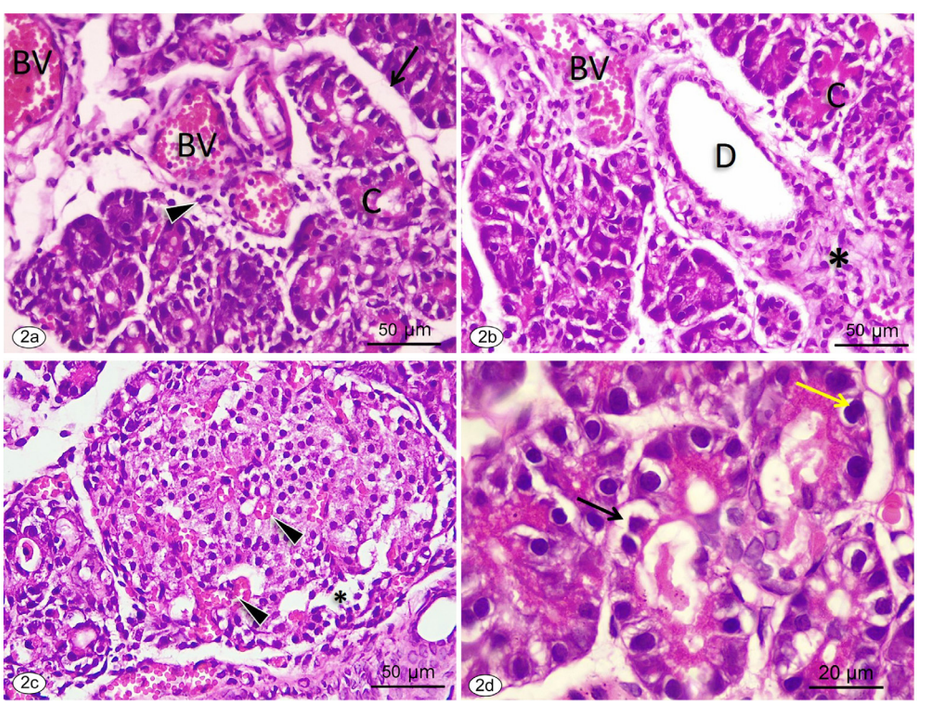

Fig. 2(a-d): Photomicrographs of a section of rat's pancreas of group2 demonstrating (a): thick interlobular CT septae (arrow), mild vascular congestion (BV) and mild perivascular inflammatory cell infiltrate (arrowhead). The acini (C) are visible. (b): the interlobular duct is mildly dilated (D) with mild periductal inflammatory cell infiltrate (*). The acini(C) and congested blood vessels (BV) are visible. (c): The Langerhans islet is apparently normal but mildly congested blood capillaries (arrowhead) and few vacuolated islet cells (*) are distinguished. (d): some acini appear merged. The acinar cells show cytoplasmic vacuolation (dark arrow) and darkly stained nuclei (yellow arrow) (H&E. a, b & c=x400, d=x1000).

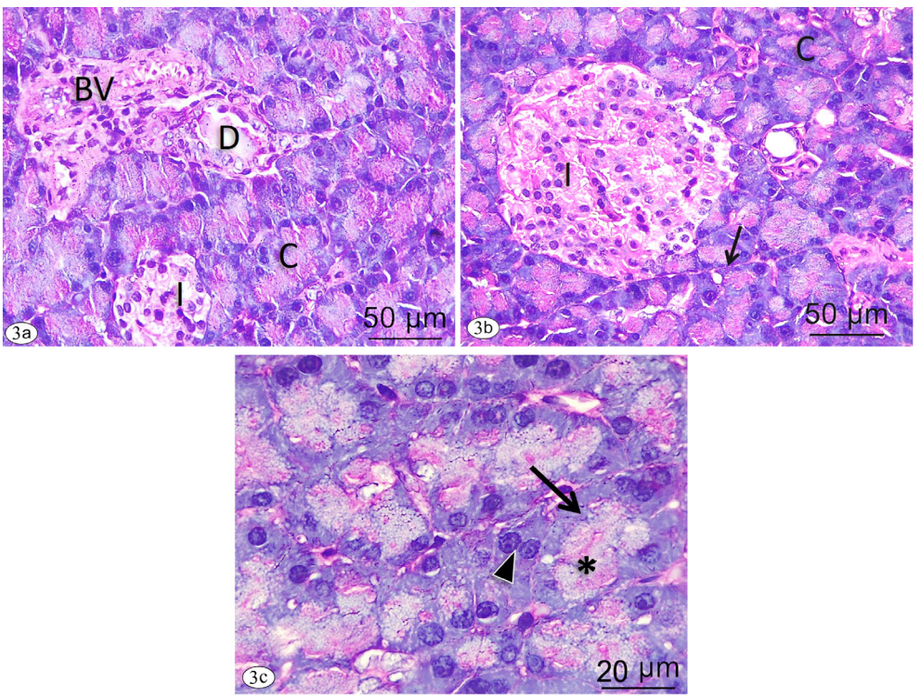

Fig. 3(a-c): Photomicrographs of a section of rat's pancreas of group3 demonstrating (a-b): restored normal construction of the acini(C), the Langerhans islets(I), the interlobular CT septae (thin arrow), ducts (D) and blood vessels (BV). The acinar cells exhibit basal rounded vesicular nuclei (arrowhead) with basal basophilic (thick arrow) and apical faint acidophilic (*) cytoplasm (H&E. a, b x400, c=x1000).

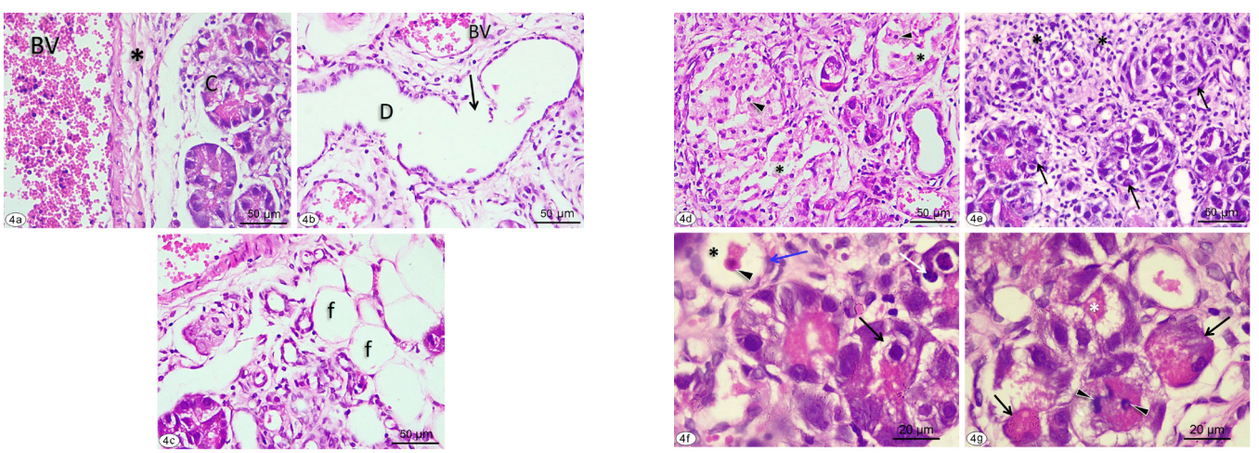

Fig. 4(a-f): Photomicrographs of a section of rat's pancreas of group4 demonstrating (a): the blood vessels (BV) are severely dilated, congested and surrounded by thick CT (*). The acini(C) are apparently reduced in number. (b): the interlobular duct (D) is greatly distended, thin walled and irregular. A tear (arrow) in its wall is seen. Congested blood vessels (BV) are observed. (c): necrotic fat cell aggregate (F) is visible. (d): most cells of Langerhans islets exhibit vacuolated cytoplasm and small darkly stained nuclei(arrowhead). Other cells show complete cytoplasmic lysis leaving empty spaces (*).(e): the acini (arrow) are severely degenerated, necrotic with disturbed cytoarchitecture. Diffuse interstitial inflammatory cell infiltrate (*) is obvious. (f): some acinar cells show cytoplasmic vacuolation (black arrow) and pyknotic nuclei (white arrow). Other cells show flattened nuclei (blue arrow), wide acinar lumen (*) containing necrotic exfoliate (arrowhead). (g): some acinar cells show cytoplasmic (*) and nuclear (arrowhead) fragmenting meanwhile others are severely shrunken (arrow) ((H&E. a, b,c,d&e x400, f&g=x1000).

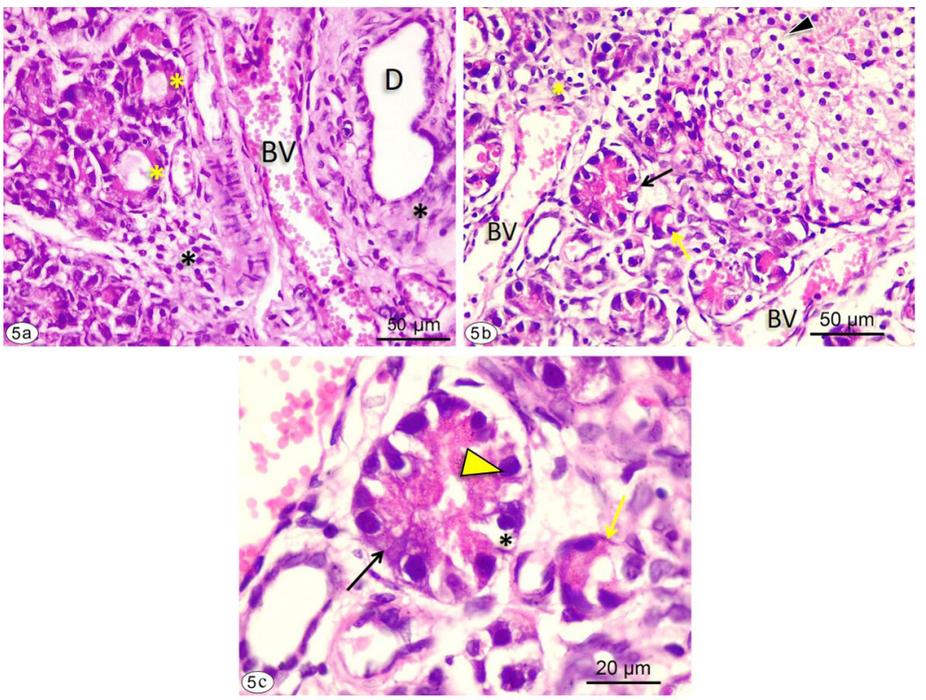

Fig. 5(a-cv): Photomicrographs of a section of rat's pancreas of group 5 demonstrating (a): mild interlobular vascular congestion (BV), ductal dilatation (D) with surrounding mild inflammatory cell infiltrating (black*). Some acini exhibit wide lumina (yellow*). (b,c): the Langerhans islet is seeming normal but some islet cells exhibit cytoplasmic vacuolation (black arrowhead). Mild intestinal inflammatory infiltrate (yellow*) is observed. Some acini (black arrow) restore normal cytoarchitecture but the acinar cells exhibit cytoplasmic vacuolations (black*) and darkly stained nuclei (white arrowhead) but other acini (yellow arrow) are shrunken. (H&E. a&b=x400, c=x1000).

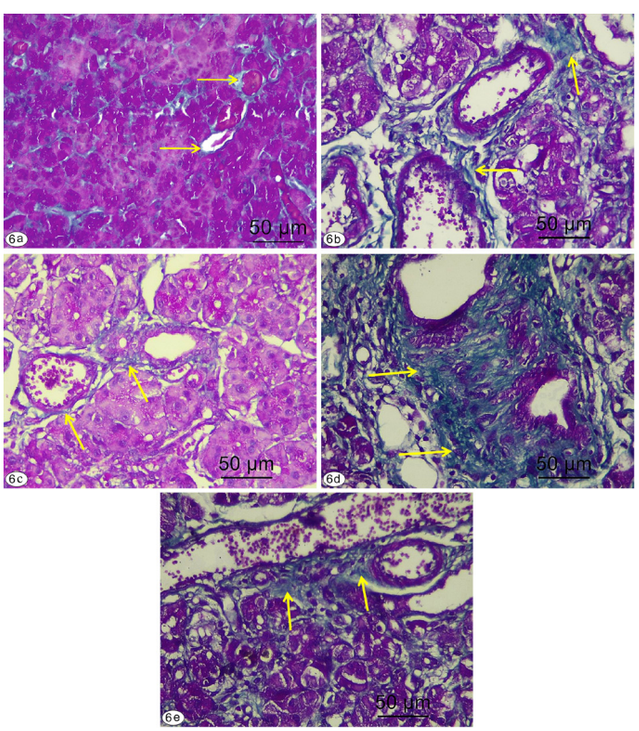

Fig. 6(a-f): Photomicrographs of MT staining sections of rat's pancreas in the different studied groups demonstrating (a): in group1, a small amount of collagen fiber deposition around the interlobular ducts and blood vessels.[b): in group2, mildly increased collagen fiber deposition contrasted to the control group (c): in group3, a marked improvement comparable to group2 and a little collagen fibers amount is distinguished. (d): in group4, an extensively dense collagen fiber deposition is obvious upon comparing with other groups (e): in group5, an obvious improvement is displayed when comparing with group 4 manifested by decreased collagen fiber deposition. Collagen fibers (yellow arrow). (MTx400)

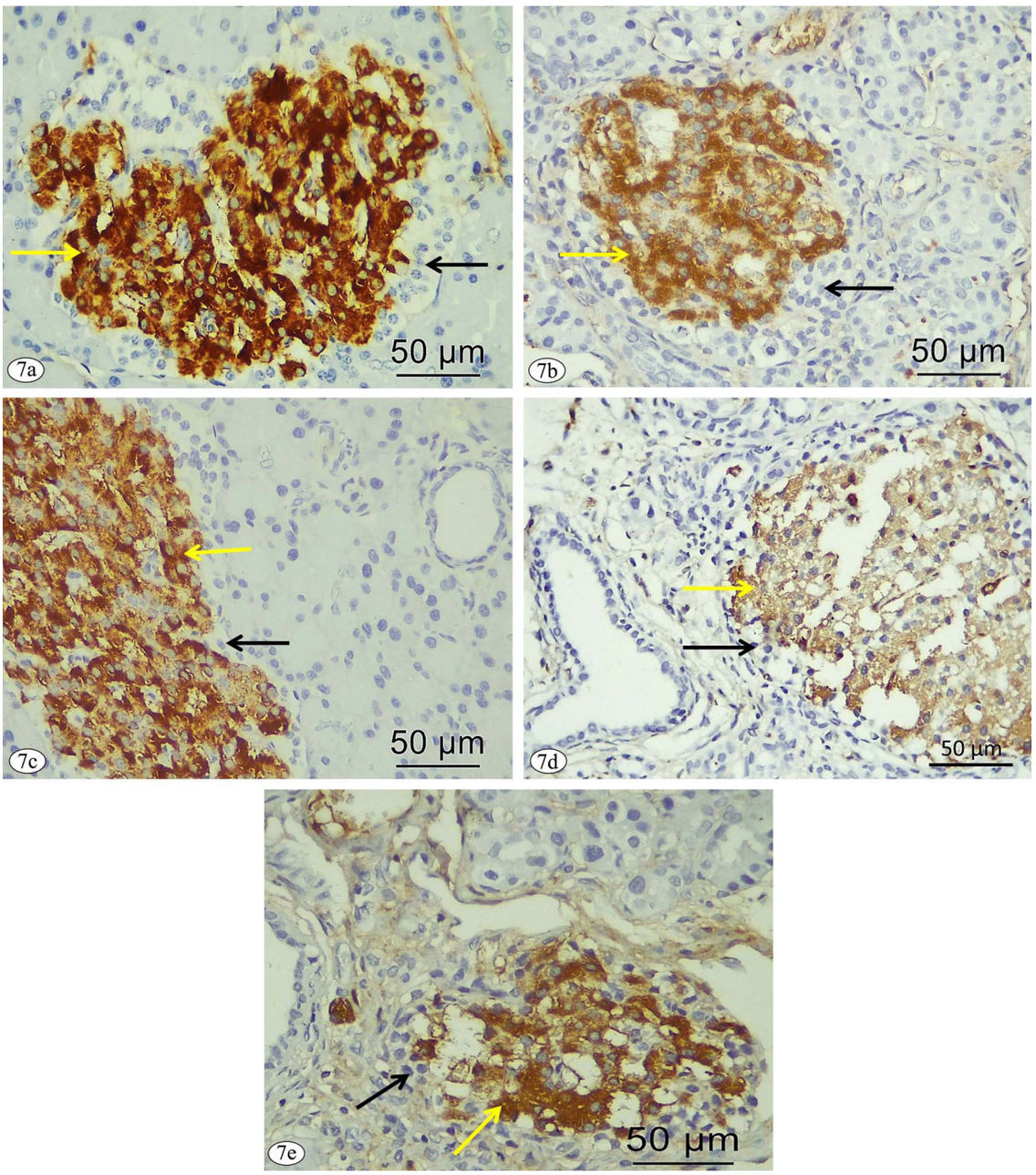

Fig.7(a-e): Photomicrographs of pancreatic sections from the different studied groups stained with anti-insulin immunostaining demonstrating B cells of Langerhans Islets (yellow arrows) in both groups1&3(a, c) exhibiting a strong positive reaction for anti-insulin antibodies seen as dark brown granules in B cell cytoplasm. In both groups2&5 (b, e), a moderate expression is observed while those of group4 (d) show marked reduction in anti-insulin antibody immunoexpressing. The cytoplasm of non-B-cells (dark arrow) of Langerhans Islets show no reaction in whole groups (Ant-insulin immunoreactivity X 400).

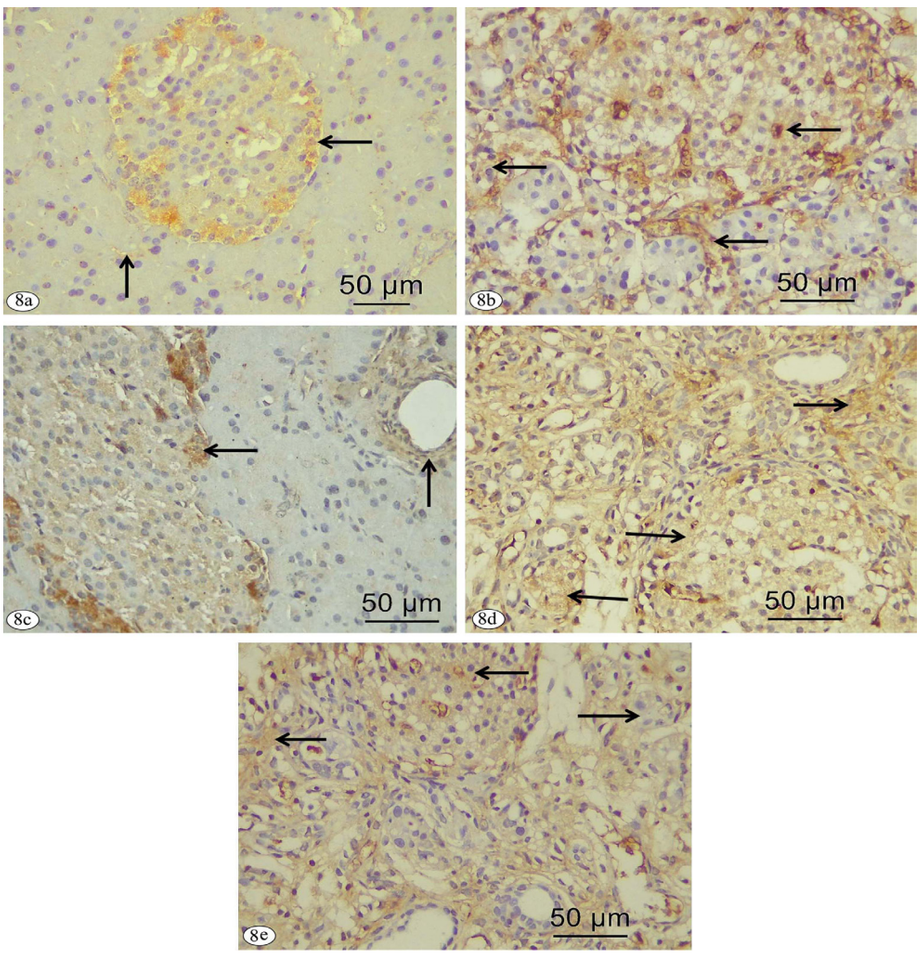

Fig. 8(a-e): Photomicrographs of immunohistochemically stained sections of the rat's pancreas from the different studied groups demonstrating in both groups1&3 (a, c) correspondingly mildly expressed caspase-3 immuno-positive reaction in the cytoplasm of both acinar and islet cells (arrows), moderately expressed in both groups2&5 (b, e) and extensive reaction in group4 (d). (Caspase-3 immunoreactivity X 400).

Table 1: The mean area % of collagen fiber deposits and positive immune reaction for Caspase and insulin immunoexpressing in the different studied groups

Parameter \ Group	Control	ZnO NPs(250mg)	ZnO NPs(250mg)+ NRG	ZnO NPs(700mg)	ZnO NPs(700mg)+ NRG	ANOVA
Collagen area %	7.66 ± 0.953	13.81 ± 4.357***	7.41 ± 1.203***	18.73 ± 3.377***	15.03 ± 1.728*	< 0.0001***
Caspase3 area %	4.80 ± 0.571	10.53 ± 1.433***	5.09 ± 0.885***	14.93 ± 2.425***	10.01 ± 1.819*	< 0.0001***
Insulin area %	46.41 ± 5.923	34.70 ± 5.444***	42.08 ± 2.646*	20.91 ± 2.098***	29.27 ± 4.241*	< 0.0001***

High significance (***) means *P value* < 0.001, Moderate significant (**) at 0.01 >*P value* >0.001 and low significance (*) when 0.05 >*P value* >0.01.

Table 1: The mean area % of collagen fiber deposits and positive immune reaction for Caspase and insulin immunoexpressing in the different studied groups

Parameter \ Group	Control	ZnO NPs(250mg)	ZnO NPs(250mg)+ NRG	ZnO NPs(700mg)	ZnO NPs(700mg)+ NRG	ANOVA
FBG (mg/dl)	85.8±7.51	84.3±7.62	85±7.1	272±23.36***	233.7± 30.95*	< 0.0001***
Amylase(U/L)	77±5.21	164.40± 6.4***	76.5± 5.24***	373.4±24.72***	299.2±29.8**	< 0.0001***
Lipase(U/L)	19.13± 1.7	31.68±1.54***	21.23±1.44***	56.78± 6.97***	47.97±5.84**	< 0.0001***
MDA (nmol/mg)	7.26±0.55	37.6±2.99***	7.73±0.71***	52.36±4.6***	46.18±4.54**	< 0.0001***

High significance (***) means *P value* < 0.001, Moderate significance (**) at 0.01 >*P value* >0.001 and low significance (*) when 0.05 >*P value* >0.01.

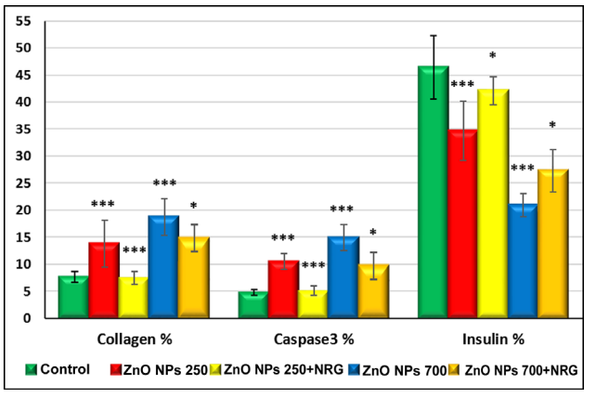

Histogram 1: The mean values of the area %of the collagen fiber deposition and area % of positive immune reaction for caspase and insulin in the different studied groups. Regarding the histogram, ZnO NPs(250mg) and ZnO NPs(700mg) groups were compared to the control group. However, ZnO NPs(250mg)+NRG was compared to the ZnO NPs(250mg) group and ZnO NPs(700mg)+NRG was compared to ZnO NPs(700mg)group.

DISCUSSION

Some earlier experimental studies indicated that, the pancreas is one of the target organs of ZnO NPs. 20-nm ZnO NPs administered orally were accumulated in the pancreas, spleen, liver, heart, and bone[13]. Also, ZnO NPs solutions with average sizes of 10-30 nm injected IP at different doses significantly affected the hepatic and pancreatic tissues with subsequent tissue and cell injury, hyperemia, inflammatory cell infiltrate, and necrosis[31]. The previous authors revealed a high ionic zinc collection in the liver and pancreas tissues with subsequent excretion into the pancreatic juice with bile. They added that, ZnO NPs detrimental impact would be due to its intra-cellular dissolution and ionic Zn2+liberation, being a heavy metal, triggering pancreatic toxicity.

Some of the pancreatic histological changes as shown by the findings of the current investigation are parallel with those of previous studies, who reported degeneration, inflammation, hyperemia, inflammatory cell infiltrate, necrosis, fibrosis and fat necrosis[13,16,31].

Also, the findings of the present study displayed ZnO NPs induced significantly raised serum amylase and lipase levels, increased MDA and caspase immunoexpressing besides declined insulin immunoexpressing. These findings together were indicative that ZnO NPs have a negative influence on the rat pancreas both structurally and functionally and this impact was dose dependent.

Furthermore, the histological alterations demonstrated in the current work were in accordance with the findings revealed by[42] in drug-induced acute pancreatitis in rats predicting that, ZnO NPs pancreatic injurious influence could be manifest as pancreatitis.

This suggestion was strengthened by the high significantly raised serum amylase and lipase levels in ZnO NPs treated rats comparing with the group of control. It has been evidenced that, elevated serum amylase and, or lipase level is a diagnostic test for acute pancreatitis[43].

With the same context, in rats and mice, exposure to excess oral zinc supplement resulted in pancreatic acinar tissue degeneration and replacement by CT[44,45]. Furthermore, ZnO NPs taken orally by mice for 2 weeks led to a high episode of pancreatitis[46].

Findings in the current study demonstrated that, ZnO NPs induced both acinar and B-cell cytoplasmic vacuolation. This might be due to impaired autophagy 2ry to lysosomal dysfunction. Autophagy is an intracellular path in which lysosome- mediated degradation and recycling of cellular organelles could occur. Thus, lysosomal disfunction with resulting impaired autophagy might be an initial event in pancreatitis induction[47].

In addition, the demonstrated pancreatic vascular dilatation and congestion in ZnO NPs treated rats would be a frequent damage following 1ry acinar cell injury and also, a constituent of an inflammatory response[43].

In the present investigation, the illustrated ZnO NPs fat necrosis could be 2ry to pancreatic lipase liberation from injured acinar cells with subsequent fat cell enzymatic devastation[48]. Furthermore, the demonstrated ZnO NPs induced ductal dilatation would be an outcome of main ductal blockage or due to a 1ry injury to ductal and interstitial cells. More frequently, it is thought to develop 2ry to widespread acinar cell injury and atrophy, acinar shrinking with subsequent pancreatic lobular atrophy leaving looser CT and dilated ducts[43].

In the current study, ZnO NPs provoked interstitial inflammatory cellular infiltration. This could be 2ry to microvascular leak besides increased interstitial leukocytic migration in cases of acute inflammation[43]. In addition, it might be 2ry to ZnO NPs provoked lymph nodal inflammation and subsequent acceleration of G 1 phase lymphocytic inflammation reaction transportation to S phase cell division[15].

The current work demonstrated ZnO NPs persuaded pancreatic fibrosis confirmed by the high significantly raised mean area % of collagen fiber deposition. This fibrosis would be attributed to pancreatic stellate cell activation. Stellate cells are inactive lipid-containing cells, triangular-shaped, located primarily round blood vessels and could be distinguished in both human and rat's pancreas. They have a vital role in pancreatic fibrosis progressing.

When these cells are triggered, lipid droplets become lost, fibroblast-like morphological appearance is gained and become capable of manufacturing collagen types I and II and migrating to peri acinar zones. The collagen fibers synthesized by stellate cells are chiefly induced by either oxidative stress or by the release of numerous interleukins, cytokines, and growth factor-a complex from a chronic cellular infiltrate. Thus, it could be suggested that, excess fibrosis would be the leading factor in acinar cytoarchitecture distortion[49].

Regarding the endocrine pancreas, IP injection of 700mg ZnO NPs induced B-cell cytotoxicity manifest as cytoplasmic vacuolation, pyknosis and occasional cytoplasmic lysis. Besides, a high significantly raised caspase3, FBG level and declined anti-insulin immunoexpressing comparable to other groups. Such findings are in accord with[15]. In addition, similar observations were noticed during diabetes mellitus, glucose toxicity, and in oxidating stress[50,51].

The previous authors clarified that; B-cells are primarily vulnerable to more oxidating stress due to their minor antioxidant enzymatic expression levels. They added that, this vulnerability could be included in B-cell histopathological alterations, disfunction development and glucose toxicity. Moreover,[52] added that, if B-cells lack insulin response, the pancreas would not be capable of insulin secretion with a subsequent rise in the blood glucose level.

In the present investigation, ZnO NPs resulted in acinar cell necrosis. This alteration might reflect a recent toxic pancreatic injury with a protein synthesis cessation. Necrosis could be elicited by toxins that attack mitochondria, endoplasmic reticulum and nucleus with subsequent disruption of their function[53].

Findings in the present work demonstrated that ZnO NPs exhibited acinar cell apoptosis manifest as acinar cell shrinking, nuclear condensing, and cytoplasmic and nuclear fragmenting. These results were enforced by the highly significantly raised mean area % of caspase immunoexpressing (a marker of apoptosis) comparable to the group of control.

Apoptosis might be a result of ZnO NPs induced intracellular stress[54] followed by mitochondrial ballooning, endoplasmic reticulum distension and lysosomal breakage and subsequent nuclear shrinking and fragmenting[55].

Apoptosis is a composite biological process of cell death program significant for cell persistence by getting rid of unhealthy cells. It is frequently applied to any cell death type, regardless of the originated mechanism. Caspase-3, being a well-known apoptosis marker, could be triggered by both intrinsic and extrinsic apoptotic ways with resultant DNA breakage[56].

In the present work, a dose dependent significantly raised pancreatic MDA level was determined in rats upon exposure to ZnO NPs denoting elevated lipid Peroxiding resulting from oxidating stress and excess ROS generation.

lipid Peroxiding is a molecular mechanism in which cellular lipid macromolecular oxidation could be accelerated with subsequently increased MDA generation[57]. Similarly, results of present study are online with[58,59,31] who proved lipid peroxiding as a molecular mechanism involved in ZnO NPs induced cell injury and toxicity. Furthermore, current results coincide with a previous investigation in which MDA level was raised in heavy metal toxicity such as mercury, chromium and silver treated mice[60].

It has been suggested that, several mechanisms were implicated in ZnO NPs induced pancreatic toxicity. ZnO NPs intra-cellular dissolution with ionic Zn2+liberation and physical ZnO NPs interaction were documented as chief mechanism triggering pancreatic toxicity[31].

A high Zn2+ concentration is cytotoxic though a low level is useful for maintaining cellular integrity[61].

Previous studies attributed ZnO NPs injurious effect to ROS mediated heavy metal toxicity. ZnO NPs dissolution, intracellular Zn2+ release, rapid Zn2+ cellular influx, fast decline in mitochondrial membrane potential, caspase- mediated apoptosis activation, mitochondrial ROS generation, excess intracellular ROS release, cell membrane injury, cell degenerative changes and finally cell death, all were included in ZnO NPs cytotoxicity[62-66].

Furthermore, oxidative stress and excess ROS release could initiate adoption cascade with succeeding pro-inflammatory cytokines liberation that induce inflammation (defensive reaction) leading to further ROS manufacture from inflammation cells with a resulting vicious circle[25].

Further probable mechanism concerning ROS generation via ZO NPs themselves is depending on the physicochemical properties of these NPs which spontaneously generate ROS on their surfaces[67]. Small sized NPs could induce more oxidating stress by disturbing the oxidant - antioxidant balance than larger ones[68].

Findings in the current work revealed that, NRG administration alleviated ZnO NPs induced pancreatic structural and functional toxicity with a great recovery regarding ZnO NPs (250mg-treated) group but partial improvement concerning ZnO NPs (700mg-treated) group was accomplished.

NRG is a flavonoid belonging to the flavanones subclass. It is broadly distributed in several Citrous fruits, grapefruit, oranges, bergamot orange, tomatoes, and additional fruits. Several studies have proved a preventive therapeutic impact of NRG.

NRG has an antioxidant and anti-inflammation characterization. Also, it could reduce pro-inflammatory factors production, decrease lipid peroxidation biomarkers and has a lipid-lowering effect. Moreover, NRG could enhance carbohydrate metabolism because of insulin-like properties, could raise antioxidating defenses and scavenge ROS. Furthermore, NRG would be able to modify immune system action, and stimulate DNA repair[69-72].

Recent studies demonstrated that, NRG formulation was modified as NRG encapsulated NPs to be utilized in the cancer chemoprevention field, in cases of liver cell failure and ulcerative colitis[73]. Also, polymeric NRG NPs were incorporated into sunscreen creams as a photoprotective and an antioxidant[74].

Findings in the present study demonstrated that, NRG administration ameliorated ZnO NPs induced pancreatic histological alterations, altered biochemical parameters

(serum amylase, lipase, blood glucose and MDA levels) and immunohistochemical changes (insulin and Caspse3 immune expression). Thus, it can be suggested that, the ameliorative effect of naringenin may be mediated via inflammation suppression, antioxidant defense system enhancement and apoptosis suppression. These findings are online with[75,76].

CONCLUSION

From the results of the present study, it could be concluded that, ZnO NPs exposure might induce a dose dependent significant detrimental histological, immunohistochemical and biochemical pancreatic alterations that may affect the function of the pancreas. This pancreatic toxicity might be due to the persuaded oxidating stress in the pancreatic tissues with subsequent tissues damage. NRG administration could ameliorate ZnO NPs toxicity either partially or completely according to the dose of ZnO NPs exposure. This amelioration might be due to NRG anti-inflammation, anti-apoptosis and anti-antioxidating characterization.

In addition, the current work results might be significant as a health risk to people who are continuously exposed to ZnO NPs and may raise alarms regarding potential risk on human well-being.More effort is required to clarify ZnO NPs potential risks on vital organs and their pathogenesis.

Our recommendation is to pay more consideration concerning ZnO NPs usage and dosage. NRG therapy would be valuable to protect against ZnO NPs accidental exposure.

CONFLICTS OF INTERESTS

There are no conflicts of interest.

REFERENCES

1. Jolanta Pulit-Prociak J, Chwastowski J, Kucharski A, Banach M. Functionalization of textiles with silver and zinc oxide nanoparticles. Appl Surf Sci 2016; 385 (1):543-553.
2. Lin CC, Lin WH, Li YY. Synthesis of ZnO nanowires and their applications as an ultraviolet photodetector. J Nanosci Nanotechnol 2009; 9(5): 2813-2819.
3. Osmond MJ, McCall MJ. Zinc oxide nanoparticles in modern sunscreens: an analysis of potential exposure and hazard. Nanotoxicology 2010; 4(1): 15-41.
4. Joh D, Kinder J, Herman L, Ju S, Segal M, Johnson J, Chan Garnet K and Park J. Single-walled carbon nanotubes as excitonic optical wires. Nat Nanotechol 2011; 6: 51–56.
5. Rasmussen JW, Martinez E, Louka P, Wingett DG Zinc oxide nanoparticles for selective destruction of tumor cells and potential for drug delivery applications. Expert Opin Drug Deliv 2010; 7: 1063-1077.
6. Wu C and Huanga Q. Synthesis of Na-doped ZnO nanowires and their photocatalytic properties. Journal of Luminescence 2010;130(11): 2136–2141.
7. Hong H, Wang F, Zhang Y, Graves SA, Eddine SB, Yang Y, Theuer CP, Nickles RJ, Wang X, Cai W. Red fluorescent zinc oxide nanoparticle: a novel platform for cancer targeting. ACS Appl Mater Interfaces 2015; 7(5): 3373-3381.
8. Bisht G, Rayamajhi S. ZnO Nanoparticles: A Promising Anticancer Agent. Nanobiomedicine 2016; 3:9 | doi: 10.5772/63437.
9. Cho W S, Duffin R, and Thielbeer F. Zeta potential and solubility to toxic ions as mechanisms of lung inflammation caused by metal/metal oxide nanoparticles. Toxicol Sci 2012;126, 469–477.
10. Choi SJ, Lee J, Jeong J, Choy JH: Toxicity evaluation of inorganic nanoparticles: considerations and challenges. Mol Cell Toxicol 2013; 9(3): 205-210.
11. Seung H.: Rat pancreatitis produced by 13-week administration of zinc oxide nanoparticles: bio persistence of nanoparticles and possible solutions. J Appl Toxicol 2013; 4: 102-110.
12. Espanani HR, Fazilati M, Sadeghi L, Yousefi BV, Bakhshiani S, Amraie E. Investigation the zinc oxide nanoparticle's effect on sex hormones and cholesterol in rat. Int Res J Biol Sci 2013; 2(8): 54-58.
13. Wang B, Feng WY, Wang M, Wang TC, Gu YQ, Zhu MT, Ouyang H, Shi JW, Zhang F, ZhaoYL, Chai ZF, Wang HF, Wang J. Acute toxicological impact of nano and submicro-scaled zinc oxide powder on healthy adult mice. J Nanopart Res 2008; 10: 263-276.
14. Al Mansour M I, Alferah MA, Shraideh A Z, Jarrar BM. Zinc oxide nanoparticles hepatotoxicity: Histological and histochemical study. Environmental Toxicology and Pharmacology 2017,;51:124–130.
15. Saman S, Moradhaseli S, Shokouhian A, Ghorbani M. Histopathological effects of ZnO nanoparticles on liver and heart tissues in wistar rats. Adv Biores 2013; 4(2): 83-88.
16. Seok SH, Cho WS, Park JS, *et al*. Rat pancreatitis produced by 13-week administration of zinc oxide nanoparticles: Biopersistence of nanoparticles and possible solutions. J Appl Toxicol 2013; 33(10): 1089-1096. [http://dx.doi.org/10.1002/jat.2862] [PMID: 23408656].
17. Kim YR, Park JI, Lee EJ, *et al*. Toxicity of 100 nm zinc oxide nanoparticles: A report of 90-day repeated oral administration in Sprague Dawley rats. Int J Nanomedicine 2014; 9(2) (Suppl. 2): 109-126.
18. Ko JW, Hong ET, Lee IC, *et al*. Evaluation of 2-week repeated oral dose toxicity of 100 nm zinc oxide nanoparticles in rats. Lab Anim Res 2015; 31(3): 139-147. [http://dx.doi.org/10.5625/lar.2015.31.3.139] [PMID: 26472967]

19. Attia H, Nounou H and Shalaby M. Zinc Oxide Nanoparticles Induced Oxidative DNA Damage, Inflammation and Apoptosis in Rat's Brain after Oral Exposure.2018Toxics, 6, 29; doi:10.3390/toxics6020029.
20. Cho WS, Duffin R, Howie SE, *et al*. Progressive severe lung injury by zinc oxide nanoparticles; the role of Zn2+ dissolution inside lysosomes. Part Fibre Toxicol 2011; 8: 27. [http://dx.doi.org/10.1186/1743-8977-8-27] [PMID: 21896169]
21. Li CH, Shen CC, Cheng YW, *et al*. Organ biodistribution, clearance, and genotoxicity of orally administered zinc oxide nanoparticles in mice. Nanotoxicology 2012; 6(7): 746-756. [http://dx.doi.org/10.3109/17435390.2011.620717] [PMID: 21950449]
22. Elshama SS, Osman HEH, El-Kenawy AE. Histopathological study of zinc oxide nanoparticle-induced neurotoxicity in rats. Curr Top Toxicol J 2017; 13: 95-103.
23. Abdelhalim M, Jarrar B. Gold nanoparticles administration induced prominent inflammatory, central vein intima disruption, fatty change and Kupffer cells hyperplasia. Lipids Health Dis. 2011;10: 113.
24. Abdulhakim M, Jarrar B. Histological alterations in the liver of rats induced by different gold nanoparticles sizes, doses and exposure duration. J.Nanobiotechnol. 2012 ; 10: 5.
25. Karnakar Reddy Y, Saritha Ch, Sridhar Y, Shankaraiah P: Naringenin Prevents the Zinc Oxide Nanoparticles Induced Toxicity in Swiss Albino Mice. J Pharmacol Clin Toxicol 2014;2(1):1021.
26. Subramanian P, Arul D. Attenuation of NDEA-induced hepatocarcinogenesis by naringenin in rats. Cell Biochem Funct 2013; 31: 511-517 [PMID: 23172681 DOI: 10.1002/cbf.2929]
27. Manchope MF, Calixto-Campos C, Coelho-Silva L, Zarpelon AC, Pinho-Ribeiro FA, Georgetti SR, Baracat MM, Casagrande R, Verri WA Jr. Naringenin inhibits superoxide anion-induced inflammatory pain: role of oxidative stress, cytokines, Nrf-2 and the NO-cGMPPKG-KATP channel signaling pathway. PLoS One 2016; 11:e0153015 [PMID: 27045367 DOI: 10.1371/journal.pone.0153015]
28. Ozkaya A, Sahin Z, Dag U, Ozkaraca M. Effects of naringenin on oxidative stress and histopathological changes in the liver of lead acetate administered Rats. J Biochem Mol Toxicol 2016; 30: 243-248 [PMID: 26929248 DOI: 10.1002/jbt.21785]
29. Ahmed OM, Hassan MA, Abdel-Twab SM, Abdel AzeemMN. Navel orange peel hydroethanolic extract, naringin and naringenin have anti-diabetic potentials in type 2 diabetic rats. Biomed Pharmacotherapy 2017; 94: 197-205 [PMID: 28759757 DOI:10.1016/j.biopha. 2017.07.094]
30. Hernández-Aquino E and Muriel P : Beneficial effects of naringenin in liver diseases: Molecular mechanisms World J Gastroenterol April 28,2018; 24(16): 1679-1707.
31. Hosseini SM, Amani R, Moshrefi AH, Vahid R S, Aghajanikhah MH, Sokouti Z. Chronic Zinc Oxide Nanoparticles Exposure Produces Hepatic and Pancreatic Impairment in Female Rats. Iranian Journal of Toxicology 2020;14(3):145-153.
32. Mozaffari Z, Parivar K, Roodbari NH and Irani S. Histopathological Evaluation of the Toxic Effects of Zinc Oxide (ZnO) Nanoparticles on Testicular Tissue of NMRI Adult Mice. Advanced Studies in Biology 2015;7(6): 275 – 291.
33. Institutional Animal Care and Use Committee (IACUC), Office of Research Compliance (ORC) (2013): Non-pharmaceutical and Pharmaceutical Grade Compounds in Research Animals.https://research.iu.edu/doc/compliance/animal-care/bloomington/iub-biacuc-non-pharmaceutical-and-pharmaceutical-grade-compounds-in-research-animals.pdf
34. Nemzek J, Bolgos G, Williams, B *et al* : Differences in normal values for murine white blood cell counts and other hematological parameters based on sampling site. Inflammation Research 2001; 50: 523–527.
35. Ghanbari E , Nejati V , Khazaei, M. Improvement in Serum Biochemical Alterations and Oxidative Stress of Liver and Pancreas following Use of Royal Jelly in Streptozotocin-Induced Diabetic Rats. Cell Journal (Yakhteh), 2016; 18(3): 362-370.
36. Nasirzadeh MR, Rasouli A. Pretreatment effect of alcoholic olive leaf extract on oxidative and antioxidative enzymes status in ovariectomized rats. Int J Women's Health Reprod Sci 2016; 4(2):77-80. [DOI:10.15296/ijwhr.2016.18]
37. Suvarna SK, Layton C, Bancroft JD: Bancroft's Theory and Practice of Histological Techniques 8th Edition, ELSEVIER, Printed in China 2018:140-147
38. Mescher, A. L. 2013: Text and Atlas of Junqueira's Basic Histology, McGraw-Hill education. 13th Edition, New York, Chicago, San Francisco, London, Madrid, Mexico, New Delhi, Sydney, Toronto. (Chapter 1) Histology & Its Methods of Study pp:1-17.
39. Ramos-Vara JA, Kiupel M, Baszier T, Bliven L, Brodersen B, Chelack B, *et al*. American Association of Veterinary Laboratory Diagnosticians Subcommittee on Standardization of Immunohistochemistry. Suggested guidelines for immunohistochemical techniques in veterinary diagnostic laboratories. J Vet Diagn Invest 2008; 20(4):393–413.

40. El-Haleem MRA, Soliman HM, El Motteleb DMA. Effect of experimentally induced portal hypertension on the fundic mucosa of adult male albino rats and the possible protective role of quercetin supplementation: histological, immunohistochemical, and biochemical study. Egyptian Journal of Histology 2013;36(1):60–77.

41. Afifi NM. Effect of mesenchymal stem cell therapy on recovery of streptozotocin-induced diabetes mellitus in adult male albino rats: a histological and immunohistochemical study. Egyptian Journal of Histology 2012; 35(3):458–69.

42. Zhang J and Rouse R L. Histopathology and pathogenesis of caerulein-, duct ligation-, and arginine-induced acute pancreatitis in Sprague-Dawley rats and C57BL6 Mice to intake natural carotenoids. Histol Histopathol 2014; 29: 1135-1152

43. Ismail ZO, Bhayana. V. Lipase or amylase for the diagnosis of acute pancratitis? Clin Biochem 2017 Dec;50(18):1275-1280

44. Aughey E, Grant L, Furman BL, Dryden WF. The effects of oral zinc supplementation in the mouse. J Comp Pathol 1977; 87(1):1-14. [DOI:10.1016/0021-9975(77)90074-3].

45. Maita K, Hirano M, Mitsumori K, Takahashi K, Shirasu Y. Subacute toxicity studies with zinc sulfate in mice and rats. J Pestic Sci 1981; 6(3):327-36. [DOI:10.1584/jpestics.6.327]

46. Pasupuleti S, Alapati S, Ganapathy S, Anumolu G, Pully NR, Prakhya BM. Toxicity of zinc oxide nanoparticles through oral route. Toxicol. Ind. Health 2012; 28: 675–686.

47. Gukovskaya A. and Gukovsky I. Autophagy and pancreatitis. Am. J. Physiol. Gastrointest. Liver Physiol. 2012; 303:G993-G1003).

48. Franco-Pons N., Gea-Serli S. and Closa D. Release of inflammatory mediators by adipose tissue during acute pancreatitis. J. Pathol. 2010; 221:175-182.

49. Abd El-Haleem M R and Mohamed D A. The effects of experimental aflatoxicosis on the pancreas of adult male albino rats and the role of ginger supplementation: a histological and biochemical study. The Egyptian Journal of Histology 2011; 34 (3) :423-435 doi: 10.1097/EHX.0000398847.67845.55

50. Kaneto H, Kawamori D, Matsuoka TA, Kajimoto Y, Yamasaki Y. Oxidative stress and pancreatic beta-cell dysfunction. Am J Ther 2005; 12:529–533.

51. Robertson RP, Harmon JS. Diabetes, glucose toxicity and oxidative stress: a case of double jeopardy for the pancreatic islet beta cell. Free Radic Biol Med 2006; 41:177–184.

52. Fapohunda SO, Akintewe T, Olarinmoye OA, Ezekiel CN. Anti-aflatoxigenic potentials of two Nigerian herbs on albino rats. J Biol Environ Sci 2009; 3:81–90.

53. Singh, A., Bhat, T., Sharma, O., Clinical biochemistry and hepatotoxicity. J. Clin. Toxicol. 2011; S4: 001.

54. Meyer, K., Rajanahalli, P., Ahmed, M., Rowe, J., Hong, Y., Nanoparticles induces apoptosis in human dermal fibroblasts via p53 and p38 pathways. Toxicol. In *Vitro*. 2011; 25 (8), 1721–1726.

55. Johar D, Roth J, Bay G, Walker J, Kroczak T, Los M. Inflammatory response, reactive oxygen species, programmed (necrotic-like and apoptotic) cell death and cancer. Rocz. Akad. Med. Bialymst. 2004; 4: 31–39.

56. Dai C, Tang S, Deng S, Zhang S, Zhou Y, Velkov T, Li J, Xiao X. Lycopene attenuates colistin-induced nephrotoxicity in mice via activation of the Nrf2/HO-1 pathway. Antimicrob Agents Chemother 2015; 59: 579 –585

57. Roy A, Das A, Das R, Haldar S, Bhattacharya S & Haldar P K. Naringenin, a Citrus Flavonoid, Ameliorates Arsenic-Induced Toxicity in Swiss Albino Mice. Journal of Environmental Pathology, Toxicology and Oncology2014;33(3):195–204.

58. Senapati VA, Kumar A, Gupta GS, Pandey AK, Dhawan A. ZnO nanoparticles induced inflammatory response and genotoxicity in human blood cells: A mechanistic approach. Food Chem. Toxicol.;2015,85:61–70.

59. Sharma AK, Singh V, Gera R, Purohit MP, Ghosh D. Zinc Oxide Nanoparticle Induces Microglial Death by NADPH-Oxidase-Independent Reactive Oxygen Species as well as Energy Depletion. Mol. Neurobiol.; 2017, 54: 6273–6286.

60. Rungby J, Ernst E. Experimentally induced lipid peroxidation after exposure to chromium, mercury or silver: Interactions with carbon tetrachloride. Pharmacol Toxicol. 1992; 70(3):205-207. [DOI:10.1111/j.1600-0773.1992.tb00458.x]

61. Sirelkhatim A, Mahmud S, Seeni A, *et al*. Review on zinc oxide nanoparticles: antibacterial activity and toxicity mechanism. Nano-Micro Letters 2015;7(3):219–242.

62. Shrivastava R, Raza S, Yadav A, Kushwaha P, Flora S. Effects of sub-acute exposure to TiO2, ZnO and Al2O3 nanoparticles on oxidative stress and histological changes in mouse liver and brain. Drug Chem Toxicol 2014; 37(3):336-347.

63. Song W, Zhang J, Guo J, Zhang J, Ding F, Li L, *et al*. Role of the dissolved zinc ion and reactive oxygen species in cytotoxicity of ZnO nanoparticles. Toxicol Lett 2010;199(3):389-397.

64. Zhao X, Ren X Zhu R, Luo Z, Ren B. Zinc oxide nanoparticles induce oxidative DNA damage and ROS-triggered mitochondria-mediated apoptosis in zebrafish embryos. Aquat Toxicol 2016; 180:56-70.

65. Wang J, Deng X, Zhang F, Chen D, Ding W. ZnO nanoparticle-induced oxidative stress triggers apoptosis by activating JNK signaling pathway in cultured primary astrocytes. Nanoscale Res Lett 2014; 9(1): 1-12.

66. Zhao X, Wang S, Wu Y, You H, Lv L. Acute ZnO nanoparticles exposure induces developmental toxicity, oxidative stress and DNA damage in embryo-larval zebrafish. Aquat Toxicol 2013;136: 49-59.

67. Park SJ, Park YC, Lee SW, Jeong MS, Yu K-N, Jung H, *et al*. Comparing the toxic mechanism of synthesized zinc oxide nanomaterials by physicochemical characterization and reactive oxygen species properties. Toxicol Lett 2011; 207(3): 197-203.

68. Abbasalipourkabir R, Moradi H, Zarei S, Asadi S, Salehzadeh A, Ghafourikhosroshahi A et al. Toxicity of zinc oxide nanoparticles on adult male Wistar rats. Food ChemToxicol 2015; 84(17): 154-160.

69. Zobeiri M, Belwal T, Parvizi F, Naseri R, Farzaei MH, Nabavi SF, Sureda A, Nabavi SM. Naringenin and its nano-formulations for fatty liver: Cellular modes of action and clinical perspective. Curr. Pharm. Biotechnol. 2018; 19: 196–205.

70. Patel K, Singh G K, Patel DK. A review on pharmacological and analytical aspects of Naringenin. Chin J Integr Med Jul; 24(7):551-560. 2018.

71. Chen C, Wei Y, He XM, Li DD, Wang GQ, Li JJ and Zhang F. Naringenin Produces Neuroprotection Against LPS-Induced Dopamine Neurotoxicity via the Inhibition of Microglial NLRP3 Inflammasome. Activation Front Immunol, May 1;10:936. doi:10.3389/fimmu.2019.00936. 2019

72. Salehi B, Fokou V T , Sharifi-Rad M, Zucca P , Pezzani R , Martins N and Sharifi-Rad J. The therapeutic potential of Naringenin: A review of clinical trials. Pharmaceuticals, 12, 11; 2019 doi:10.3390/ph12010011

73. Neha, R.; Saurabh, B.; Bhaskar, K.; Jagriti, B.; Charu, S.; Mohammad, A.; Shreesh, O. and Dharamvir, SA. Pharmacological Properties and Therapeutic Potential of Naringenin: A Citrus Flavonoid of Pharmaceutical Promise, Current Pharmaceutical Design, (2016), 22, 1-19.

74. Joshi H, Hegde R A, Shetty K P, Gollavilli H, Managuli S R, Kalthur G, Mutalik S. Sunscreen creams containing naringenin nanoparticles: Formulation development and in *vitro* and in *vivo* evaluations. Photodermatol Photoimmunol Photomed. 2018; 34:69–81.

75. Ahmed M O, Fahim I H, Ahmed Y H, Al-Muzafar M H, Ahmed R R, Adel Amin K, El-Nahass E and Abdelazeem H W. The Preventive Effects and the Mechanisms of Action of Navel Orange Peel Hydroethanolic Extract, Naringin, and Naringenin in N-Acetyl-p-aminophenol-Induced Liver Injury in Wistar Rats. Oxidative Medicine and Cellular Longevity Volume 2019, Article ID 2745352, 19 pages https://doi.org/10.1155/2019/2745352

76. Kandemir F M, Kucukler S, Eldutar E, Caglayan C, and Gülçin İ. Chrysin protects rat kidney from paracetamol induced oxidative stress, inflammation, apoptosis, and autophagy: a multi-biomarker approach," Scientia Pharmaceutica, 2017; 85 (1) :1–12.

الملخص العربى

التأثير السمى لجزيئات أكسيد الزنك متناهية الصغر على البنكرياس والدور المحسن للنارينجينين: دراسة نسيجية وهستوكيميائية مناعية

أمل سليمان سويلم ومحمد أحمد شحاته أمين

قسم التشريح والأجنة- كلية الطب- جامعة الزقازيق، مصر

مقدمة: على الرغم من الإستخدام الكبير لجزيئات أكسيد الزنك النانوي في مجالات الطب الحيوي والهندسة الحيوية والتجميل إلا أنه قد نشأ جدلا واسعا حول فوائدها مقارنة بتأثيراتها السمية على الأنظمة البيولوجية للجسم. يعتبر النارينجينين من مضادات الأكسدة الطبيعية التابعة للفلافونويد.

هدف البحث: يهدف البحث إلى إستكشاف التغيرات النسيجية والهيستوكيميائية المناعية في بنكرياس الفئران بعد الحقن بجرعتين مختلفتين من جزيئات أكسيد الزنك النانوي الذى حجمه ٣٥ نانومتر داخل الغشاء الصفاقى ولتقييم الدور المحسن للنارينجينين.

المواد والطرق المستخدمة: أستخدم فى هذا البحث خمس وأربعون من ذكور الفئران البيضاء البالغة حيث تم تقسيمهم بشكل عشوائى الى خمس مجموعات. أعتبرت المجموعة الأولى ضابطة. أما المجموعتان الثانية والرابعة فقد تم حقنهم بجرعة واحدة من جزيئات أكسيد الزنك النانوي داخل الغشاء الصفاقى بمعدل ٢٥٠و ٧٠٠ مجم لكل كيلو جرام من وزن الجسم على التوالى. أما المجموعاتان الثالثة والخامسة فقد تم حقنهم بنفس الجرعات السابقة من جزيئات أكسيد الزنك النانوى على الترتيب بالإضافة الى تجريع الفئران لمادة النارنجنين بمعدل ٢٠ مجم لكل كيلوجرام من وزن الجسم عن طريق الفم مرة واحدة يوميا لمدة أربعة عشر يوما متتالية. و قد أخذت عينات من الدم لتحليلها وكذلك تم قياس معايير هستولوجية وهستوكيميائية مناعية مختلفة من أنسجة البنكرياس المأخوذة من جميع الحيوانات قيد الدراسة قبل التضحية بها.

النتائج: وقد وجد ان المجموعات التى تم معالجتها بجزيئات أكسيد الزنك النانوى قد أظهرت تلفًا خلويًا يتجلى في احتقان الأوعية الدموية واتساع القنوات والتليف وتسلل الخلايا الالتهابية. كما أظهرت كل من الخلايا الأسينار والخلايا البائية تغيرات تباينت من كونها فجوات حشوية في الجرذان المعالجة ب٢٥٠ مجم من جزيئات أكسيد الزنك النانوى إلى التقلص الشديد في الخلايا والتفتت السيتوبلازمي والنووي في الفئران المعالجة بـ ٧٠٠ مجم من جزيئات أكسيد الزنك النانوى. علاوة على ذلك فقد حدثت زيادة كبيرة في متوسط النسب المئوية لترسب ألياف الكولاجين والتعبير المناعي للكاسباس. كما ارتفع مستوي الجلوكوز الصائم في الدم وكذلك نسب الأميليز والليباز و المالوندايالدهيد إلى جانب الإنخفاض في متوسط النسب المئوية للتعبير المناعي للأنسولين مقارنة بالمجموعة الضابطة .إزدادت هذه التغيرات تبعا لإزدياد جرعة أكسيد الزنك النانوى.

الخلاصة: من المحتمل أن تسبب جزيئات أكسيد الزنك النانوى سمية هيكلية ووظيفية في بنكرياس الفئران عن طريق الإجهاد المؤكسد مع قابلية التحسن الكبير بواسطة المعالجة المتزامنة بالنارينجينين. يوصى بعمل مستقبلي يشمل سمية جزيئات أكسيد الزنك النانوى على الأعضاء الحيوية ودور النارينجينين في مقاومة هذا التأثير.